

# A Data Driven Neural Network Approach to Optimal Asset Allocation for Target Based Defined Contribution Pension Plans

Yuying Li\*      Peter Forsyth†

June 6, 2018

## Abstract

A data driven Neural Network (NN) optimization framework is proposed to determine optimal asset allocation during the accumulation phase of a defined contribution pension scheme. In contrast to parametric model based solutions computed by a partial differential equation approach, the proposed computational framework can scale to high dimensional multi-asset problems. More importantly, the proposed approach can determine the optimal NN control directly from market returns, without assuming a particular parametric model for the return process. We validate the proposed NN learning solution by comparing the NN control to the optimal control determined by solution of the Hamilton-Jacobi-Bellman (HJB) equation. The HJB equation solution is based on a double exponential jump model calibrated to the historical market data. The NN control achieves nearly optimal performance. An alternative data driven approach (without the need of a parametric model) is based on using the historic bootstrap resampling data sets. Robustness is checked by training with a blocksize different from the test data. In both two and three asset cases, we compare performance of the NN controls directly learned from the market return sample paths and demonstrate that they always significantly outperform constant proportion strategies.

**Keywords:** DC plan asset allocation, data-driven, neural network, target based objective

**JEL classification:** C61, D81, G11, G22

## 1 Introduction

Throughout the Western world, it is clear that there is a major paradigm shift away from defined benefit (DB) pension plans to defined contribution (DC) plans. Both the public and private sectors are no longer willing to take on the risk of DB plans.

In a typical employee sponsored DC plan, employee and employer contribute to a (usually) tax advantaged account. Often, the employee is presented with a list of possible investment funds, and then required to select an asset allocation from this list. If one considers that the DC fund will be managed by the employee for 30+ years of employment, it is clear that asset allocation will be of crucial importance in order to have a reasonable level of salary replacement during the retirement (decumulation) phase.

In this article, we formulate the multi-period asset allocation strategy during the accumulation phase of a DC pension fund as an optimal stochastic control problem. We use the target based objective function advocated in (Menoncin and Vigna, 2017).

---

\*David R. Cheriton School of Computer Science, University of Waterloo, Waterloo ON, Canada N2L 3G1, yuying@uwaterloo.ca, +1 519 888 4567 ext. 37825.

†David R. Cheriton School of Computer Science, University of Waterloo, Waterloo ON, Canada N2L 3G1, paforsyt@uwaterloo.ca, +1 519 888 4567 ext. 34415.

34 It is well known (Zhou and Li, 2000; Li and Ng, 2000) that target based objective functions are equiv-  
35 alent to pre-commitment mean variance criteria. Previous work on pre-commitment mean variance asset  
36 allocation in the DC pension plan context has been based on (i) postulating a parametric stochastic process  
37 for the portfolio components, and (ii) solution of the optimal control problem via a Hamilton Jacobi Bellman  
38 (HJB) Partial Differential Equation (PDE) (Vigna, 2014; He and Liang, 2013; Yao et al., 2013; Guan and  
39 Liang, 2015).

40 We should also mention that there is a strand of literature which focuses on time-consistent mean-  
41 variance formulations (see Wu et al. (2015) for example). However, target based objective functions (since  
42 they can be solved using dynamic programming) are clearly time consistent for a fixed target value. Hence,  
43 since we are focusing on target based objective functions, the fact that the equivalent mean-variance problem  
44 is time inconsistent is not particularly relevant.

45 We should also point out that previous work on determining optimal controls for DC plan asset allocation  
46 has been mostly restricted to developing closed form solutions of the HJB equation (Vigna, 2014; He and  
47 Liang, 2013; Yao et al., 2013; Guan and Liang, 2015; Wu et al., 2015). However, this often requires making  
48 unrealistic assumptions, e.g. continuous rebalancing, infinite leverage, trading continues even if insolvent.  
49 In fact, one might question previous economic conclusions based on closed-form solutions. For example  
50 in (Lioui, 2013), the authors favour time-consistent mean variance strategies compared to pre-commitment  
51 policies, since the latter uses large leverage ratios. This problem can, of course, be eliminated by imposing  
52 realistic leverage ratio constraints.

53 In order to allow for practical considerations for DC pension plan asset allocation, such as no-shorting  
54 and no-leverage, and discrete rebalancing, numerical methods for solution of the associated HJB PDE have  
55 been developed in (Dang and Forsyth, 2014; Forsyth and Labahn, 2018).

56 In contrast to these previous approaches, we propose to use a data-driven method in this work. In other  
57 words, we operate directly on the observed historical data, and by-pass the error prone step of calibrating a  
58 parametric model to historical data.

59 In this paper, we propose a data driven machine learning approach for multi-period optimal asset al-  
60 location strategy during the accumulation phase of a DC pension fund. We remark that machine learning  
61 approaches have recently been suggested for a variety of insurance related problems (Gan and Lin, 2015;  
62 Gan, 2013; Hejazi and Jackson, 2016). In (Gan and Lin, 2015; Gan, 2013), clustering and a functional  
63 data approach have been considered for efficient valuation of portfolios of variable annuities. In (Hejazi  
64 and Jackson, 2016), Neural Network approaches are also used for fast computation of portfolios of vari-  
65 able annuities. In our proposed method, we represent the control function of the multi-period allocations  
66 as a Neural Network (NN) based on a feedback function of feature variables. Our formulation can handle  
67 constraints (i.e. discrete rebalancing, no-shorting, no-leverage) in a straightforward manner. Note that the  
68 numerical approaches for solving the HJB PDE in (Dang and Forsyth, 2014; Forsyth and Labahn, 2018) can  
69 also handle these types of constraints, but numerical PDE methods are restricted to a small ( $\leq 3$ ) number of  
70 factors. Our NN formulation, in principle, can be applied to problems having a larger number of factors.

71 We validate our approach by considering a *synthetic* market where the assets follow a known parametric  
72 stochastic process. In this case, we can compute the provably optimal asset allocation strategy by solving  
73 a Hamilton Jacobi Bellman (HJB) equation. Our data driven solution takes as input only samples from the  
74 parametric process. Remarkably, our data driven parsimonious NN approach produces results very close to  
75 the HJB solution.

76 We then test the data driven NN solution of the control problem on bootstrap resampling of the historical  
77 data, and compare with constant weight strategies. The data driven NN controls are superior in all cases to  
78 the constant weight strategies.

## 79 2 Technical Objectives

80 The objective of this paper is to propose a computational framework, which produces the optimal control  
81 for asset allocation in a long term DC pension plan portfolio. The advantages of our approach are (i) based  
82 solely on sampling price paths (no parametric model required), (ii) allows realistic constraints on the asset  
83 allocation policy (e.g. no leverage, no shorting, discrete rebalancing) and (iii) can potentially be extended to  
84 high dimensional cases (many assets, taxation effects, transaction costs).

85 More precisely, we make the following contributions:

86 • We take a machine learning approach and determine the control  $\vec{p}(\cdot, t)$ , where  $\vec{p}(\cdot, t)_k$  represents the  
87 fraction of the total investor wealth invested in the  $k^{\text{th}}$  asset at time  $t$ . The control is in feedback form,  
88 i.e., a function of current state and time. The proposed control model is a Neural Network (NN) with  
89 an input layer, a hidden layer, and an output layer. The control model is learned by solving a global  
90 optimization model defined by a set of sample paths.

91 • Using simulated samples from a parametric model estimated from monthly market data, we validate  
92 the proposed approach by comparing the performance of the optimal NN control with that of the  
93 optimal control determined from the solution of the HJB equation, in two examples with different  
94 asset pairs. The HJB solution represents ground truth in this situation.

95 We demonstrate that, using an NN of a single hidden layer with only 3 hidden nodes, the training  
96 performance of the NN control is on par with that from the HJB equation. In addition, the test results  
97 from bootstrap resampling data sets demonstrate that the NN optimal controls significantly outperform  
98 a typical constant proportion strategy, yielding a higher median wealth, and a significantly smaller  
99 risk, as measured by probability of shortfall and standard deviation, but achieving approximately the  
100 same expected wealth.

101 • Using bootstrap resampling market data sets with varying expected block sizes, in the two-asset case,  
102 we learn the NN optimal controls directly from the market return samples. Performance is tested in  
103 out-of-sample mode using returns simulated with the parametric model. The NN control similarly has  
104 a higher median wealth, with a lower risk, compared to a constant proportion strategy.

105 • We also consider 3-asset examples and learn the optimal NN strategy directly from a bootstrap resam-  
106 pling market return data set. Performance is tested in out-of-sample mode using resampling return  
107 data sets with block sizes different from the training set block size. We observe similar superior train-  
108 ing and testing performance from the NN control, compared to a constant proportion strategy. The  
109 NN control produces a higher median terminal wealth with lower risk.

## 110 3 Embedded Formulation for Dynamically Optimal Long Term Investment

111 Consider an investment problem in  $M$  risky and riskless assets whose prices  $\vec{S}_t$  follow a Markov process.  
112 Let the initial time  $t_0 = 0$  and consider a set  $\mathcal{T}$  of rebalancing times

$$\mathcal{T} \equiv \{t_0 = 0 < t_1 < \dots < t_N = T\}. \quad (1)$$

113 The fraction of total wealth allocated to each asset is adjusted at times  $t_n, n = 0, \dots, N-1$ , with the investment  
114 horizon  $t_N = T$ .

115 Assume that, at time  $t$ , a fund holds wealth of amount  $W_m(t)$  in asset  $m, m = 1, \dots, M$ . The total value of  
116 the portfolio at  $t$  is then

$$W(t) = \sum_{m=1}^M W_m(t). \quad (2)$$

117 Let  $t_n^+ = t_n + \varepsilon$ ,  $t_n^- = t_n - \varepsilon$ ,  $\varepsilon \rightarrow 0^+$ . Assume that  $W(t_0^-) = 0$ , i.e., the initial value of the portfolio is zero,  
 118 and let  $\{q(t_n)\}$  represent an *a priori* specified cash injection schedule.

119 Given an allocation control sequence  $\vec{\rho}_0, \dots, \vec{\rho}_{N-1}$ , the dependence of the terminal wealth  $W(T)$  on the  
 120 control is as follows,

$$\begin{aligned}
 & \text{for } n = 0, 1, \dots, N-1 \\
 & \quad W(t_n^+) = W(t_n^-) + q(t_n) \\
 & \quad W(t_{n+1}^-) = \vec{\rho}_n^T \vec{R}(t_n) W(t_n^+) \\
 & \quad \quad = \left( \vec{\rho}_n^T \vec{R}(t_n) \right) (W(t_n^-) + q(t_n)), \\
 & \text{end}
 \end{aligned} \tag{3}$$

121 where  $\vec{R}(t_n)$  is the vector of returns on assets in  $(t_n^+, t_{n+1}^-)$ .

122 Using the target based objective function advocated in (Menoncin and Vigna, 2017), a standard for-  
 123 mulation for the multi-period allocation problem is the following constrained quadratic optimization, with  
 124 controls  $\vec{\rho}_0(\cdot), \dots, \vec{\rho}_{N-1}(\cdot)$ , where  $\vec{\rho}_n(\cdot)$  depends only on the wealth  $W(t_n)$ ,

$$\begin{aligned}
 & \min_{\{\vec{\rho}_0(\cdot), \dots, \vec{\rho}_{N-1}(\cdot)\}} \quad \mathbf{E} \left[ (W(T) - W^*)^2 \right] \\
 & \text{subject to} \quad 0 \leq \vec{\rho}_n(\cdot) \leq 1, \quad n = 0, 1, \dots, N-1, \\
 & \quad \quad \mathbf{1}^T \vec{\rho}_n(\cdot) = 1, \quad n = 0, 1, \dots, N-1,
 \end{aligned} \tag{4}$$

125 where  $W^*$  is a given target parameter.

126 The following Proposition, proven in Zhou and Li (2000), establishes an additional appealing property  
 127 of the quadratic target formulation (4).

128 **Proposition 1** (Dynamic mean variance efficiency). *Problem (4) is multi-period mean variance optimal, in*  
 129 *the pre-commitment sense.*

130 Instead of the quadratic objective in Problem (4), in this paper, we consider

$$\begin{aligned}
 & \min_{\{\vec{\rho}_0(\cdot), \dots, \vec{\rho}_{N-1}(\cdot)\}} \quad g(W(T)) \equiv \mathbf{E} \left[ (\min(W(T) - W^*, 0))^2 \right] \\
 & \text{subject to} \quad 0 \leq \vec{\rho}_n(\cdot) \leq 1, \quad n = 0, 1, \dots, N-1, \\
 & \quad \quad \mathbf{1}^T \vec{\rho}_n(\cdot) = 1, \quad n = 0, 1, \dots, N-1.
 \end{aligned} \tag{5}$$

131 **Remark 1** (Relation of Problem (4) and Problem (5)). *In Dang and Forsyth (2016), it is shown that a*  
 132 *solution of Problem (5) is a solution of Problem (4) when the set of admissible controls is enlarged to*  
 133 *include withdrawing cash. Since the control set for Problem (5) is larger than the control set for Problem*  
 134 *(4), then the optimal value of the objective function in Problem (5) can never be larger than the optimal*  
 135 *objective function of Problem (4).*

136 Here we give an intuitive interpretation of the objective function in Problem (5). In the context of an  
 137 investor saving for retirement, we can imagine that  $W^*$  is a target value of (real) wealth at the retirement  
 138 date  $t = T$ . This objective function penalizes the expected quadratic shortfall with respect to the target  $W^*$ .  
 139 Note that we do not penalize final wealth which exceeds  $W^*$ . In other words, we measure risk only in terms  
 140 of undershooting the target wealth  $W^*$ . This is similar in spirit to the use of an upside wealth constraint  
 141 suggested in (Donnelly et al., 2015). For a discussion concerning target based strategies for DC pension  
 142 plans, we refer the reader to (Vigna, 2014; Menoncin and Vigna, 2017).

143 **Remark 2** (Time consistency). *There is considerable confusion in the literature about pre-commitment*  
144 *mean-variance strategies. These strategies are commonly criticized for being time inconsistent (Basak and*  
145 *Chabakauri, 2010; Bjork et al., 2014). However, the pre-commitment optimal policy can be found by solving*  
146 *problem (5), which can be determined by dynamic programming, and hence is time consistent when viewed*  
147 *as minimizing expected quadratic shortfall with respect to a fixed target  $W^*$ . Consequently, when deter-*  
148 *mining the time consistent optimal strategy for problem (5), we obtain, as a by-product, the optimal mean*  
149 *variance pre-commitment solution. Further insight has been provided in (Vigna, 2017) and (Vigna, 2014;*  
150 *Menoncin and Vigna, 2017). As noted in (Cong and Oosterlee, 2016), the pre-commitment strategy can be*  
151 *seen as a strategy consistent with a fixed investment target, but not with a risk aversion attitude. Conversely,*  
152 *a time-consistent strategy has a consistent risk aversion attitude, but is not consistent with respect to an*  
153 *investment target. We contend that consistency with a target is more natural for DC pension investment*  
154 *strategies.*

155 We note that Problem (5) does not uniquely specify the optimal controls. Suppose that one of the assets  
156 is a risk free bond with interest rate  $r$ . Let

$$Q(t_\ell) = \sum_{j=\ell+1}^{j=N-1} e^{-r(t_j-t_\ell)} q(t_j) \quad (6)$$

157 be the discounted future contributions as of time  $t_\ell$ . If

$$(W(t_n^- + q(t_n)) > W^* e^{-r(T-t_n)} - Q(t_n), \quad (7)$$

158 then an optimal strategy is to (i) invest  $(W^* e^{-r(T-t_n)} - Q(t_n))$  in the risk-free asset; and (ii) invest the remainder  
159  $(W^* e^{-r(T-t_i)} - Q(t_i))$  in any long positions in the stock and bond. This strategy remains optimal since, when  
160 equation (7) holds at time  $t_i^-$ , then  $\mathbf{E}[(\min(W(T) - W^*, 0))^2] = 0$  (Dang and Forsyth, 2016). As is common  
161 in the literature, we refer to the amount  $W(t_n^-) + q(t_n) - (W^* e^{-r(T-t_n)} - Q(t_n))$  as free or surplus cash (Bauerle  
162 and Grether, 2015). In the following sections, we describe a tie-breaking strategy which ensures that, if a  
163 risk-free asset is available, we invest the surplus in the risk-free asset.

## 164 **4 A Data Driven Approach Solving a Single Optimization Problem**

165 Problem (5) is an  $N$  stage stochastic optimization problem, which suffers from the curse of dimensionality.  
166 When the number of assets  $M \leq 3$ , the optimal control can be determined by solving a Hamilton-Jacobi-  
167 Bellman (HJB) equation (Dang and Forsyth, 2014; Forsyth and Labahn, 2018). Unfortunately, for a larger  
168  $M$ , a sample based approximation is necessary and some approximate dynamic programming algorithm  
169 needs to be used.

170 Assume that the price  $\vec{S}(t_n)$  follows a Markov process and the objective function  $g(W(T))$  is regarded as  
171 a cost/reward function for the control policy. The asset allocation problem (5) can be solved approximately  
172 by reinforcement learning (RL)/backward dynamic programming (DP) methods, for which samples from  
173 the Markov process are specified (Bertsekas and Tsitsiklis, 1996). This gives rise to a finite horizon and  
174 continuous space optimization problem, which can be solved with an approximate DP/RL approach, via  
175 either forward or backward iterations, using a policy iteration or value iteration method. Bellman's principle  
176 is the crucial foundation for both types of methods since it converts the optimal selection of a sequence  
177 of decisions to a sequence of selections of decisions. In particular, value iteration algorithms search for  
178 optimal value functions, which are then used to compute optimal policies. Policy iteration methods, on the  
179 other hand, iteratively improve controls and the value function of the current control is determined and used  
180 to compute new policies.

181 Instead of following the typical approach to solve (5) sequentially using Bellman's equation, we propose  
 182 to solve this multi-stage optimization problem directly from sample paths by seeking a global function  
 183  $\vec{p}(F(t_n)) \in \mathfrak{R}^M$  of the state  $F(t_n)$ , for  $n = 0, 1, \dots, N-1$ , where  $F(t_n)$  is a feature vector, representing the  
 184 information needed to determine the control at  $t_n$ , including minimally the current wealth at time  $t_n$  and  
 185 time to go  $T - t_n$ . The objective is to minimize a performance measure  $g(W(T))$  based on the terminal  
 186 wealth at  $T$ . In other words, instead of selecting  $N$  control functions in (5), which are multiple functions  
 187 of current wealths, e.g., in (4) and (5), we seek a single function  $\vec{p}(\cdot)$  of the feature vector  $F(t_n)$ , with time  
 188 explicitly included as a feature variable of time-to-go  $T - t_n$ . By using a global model  $\vec{p}(\cdot)$  to represent  
 189 controls at different time  $t_n$  through a time-to-go feature variable, we leverage continuity of the control with  
 190 respect to time, which enhances learning efficiency. In addition, solving a global control model in a single  
 191 optimization, instead of using the Bellman's equation, avoids error propagation, which is unavoidable in the  
 192 iterative time stepping process. Indeed our computational results, based on both synthetic and real data, will  
 193 validate the proposed approach.

194 Let  $\vec{p}(F(t))$  be the vector of controls at time  $t$ , which depends on the feature vector  $F(t)$ . At each  
 195 rebalancing time  $t_n$ , the control function  $\vec{p}(F(t_n)) \in \mathfrak{R}^M$  yields fractions of the total wealth to be allocated to  
 196  $M$  assets. In other words, we let  $\vec{p}_n(W(t_n)) = \vec{p}(F(t_n))$  and the amount invested in asset  $m$  is

$$W_m(t_n^+) = \vec{p}(F(t_n))_m W(t_n^+), \quad (8)$$

197 so that the the vector of asset wealths at  $t_n^+$ , is

$$\vec{p}(F(t_n))W(t_n^+) = \vec{p}(F(t_n))(W(t_n^-) + q(t_n)). \quad (9)$$

198 Hence the wealth amount vector, after rebalancing at  $t_n$ , is  $\vec{p}(F(t_n))W(t_n^+)$ .

199 Given a control sequence  $\vec{p}(F(t_0)), \dots, \vec{p}(F(t_{N-1}))$ , the dependence of the terminal wealth  $W(T)$  on the  
 200 control  $\vec{p}(F(t_0)), \dots, \vec{p}(F(t_{N-1}))$  now becomes,

$$\begin{aligned} \text{for } n = 0, 1, \dots, N-1 \\ W(t_n^+) &= W(t_n^-) + q(t_n) \\ W(t_{n+1}^-) &= \vec{p}(F(t_n))^T \vec{R}(t_n) W(t_n^+) \\ &= \left( \vec{p}(F(t_n))^T \vec{R}(t_n) \right) (W(t_n^-) + q(t_n)) \end{aligned} \quad (10)$$

end

201 where  $\vec{R}(t_n)$  is the (stochastic) vector return on assets in  $(t_n^+, t_{n+1}^-)$ . The final wealth  $W(T) = W(t_N^-)$ . For  
 202  $t \in (t_n^+, t_{n+1}^-)$ ,  $W(t)$  follows a stochastic process determined by  $\vec{S}_t$  and hence the feature vector  $F(t)$  is also  
 203 stochastic.

204 Corresponding to (5), we have the following optimal investment problem seeking a global control func-  
 205 tion,

$$\begin{aligned} \min_{\vec{p}(\cdot)} \quad & g(W(T)) \\ \text{subject to} \quad & 0 \leq \vec{p}(F(t_n)) \leq \mathbf{1}, \quad n = 0, 1, \dots, N-1, \\ & \mathbf{1}^T \vec{p}(F(t_n)) = 1, \end{aligned} \quad (11)$$

206 where the bound constraints specify no shorting and no leverage respectively, which would be common in  
 207 practice.

208 Solving the multi-dimensional stochastic dynamic programming problem (11) remains computationally  
 209 challenging when the number of asset  $M$  is large, particularly when we are interested in solving a long

210 horizon investment problem, e.g.,  $N = 30$  years. Note that the feature vector  $F(t)$  takes on continuous  
 211 values, and that the control  $\vec{p}(F(t))$  depends on the feature  $F(t)$ . Hence, in order to use stochastic dynamic  
 212 programming, we need to sample from the continuous state space  $F(t)$ . Of course, practical problems also  
 213 necessitate honouring the constraints in Problem (11). In the learning context,  $F(t)$  could be any features,  
 214 representing relevant information available at  $t$ , which are used to train the model.

215 When solving the multi-asset problem (11) with  $M > 3$ , a sample based approach is likely the only viable  
 216 computationally feasible approach. The idea is then to learn the optimal control function  $\vec{p}(\cdot)$  based on the  
 217 available sample paths, which come from either simulations of a parametric model or more interestingly,  
 218 return samples observed directly from the market. In the latter case, we are then learning the optimal control  
 219 directly from the market, bypassing an intermediate parametric modeling step, which has been the common  
 220 practice in financial modeling.

221 Specifically, assume that a set of  $L$  return sample paths  $\{\vec{R}^{(j)}(t_n), n = 1, \dots, N, j = 1, \dots, L\}$  are given. Let  
 222  $\vec{p}^{(j)}(F(t_n))$  denote the allocation at time  $t_n$  along the  $j^{\text{th}}$  path. This yields the sample optimization problem  
 223 below, arising from equation (11) based on samples,

$$\begin{aligned} \min_{\{\vec{p}(F^{(j)}(t_0)), \vec{p}(F^{(j)}(t_1)), \dots, \vec{p}(F^{(j)}(t_{N-1}))\}} & \frac{1}{2} \bar{g}(W^{(1)}(T), \dots, W^{(L)}(T)) & (12) \\ \text{subject to} & 0 \leq \vec{p}(F^{(j)}(t_n)) \leq 1, \quad n = 0, 1, \dots, N-1, j = 1, \dots, L, \\ & \mathbf{1}^T \vec{p}(F^{(j)}(t_n)) = 1, \quad n = 0, 1, \dots, N-1, j = 1, \dots, L, \end{aligned}$$

where  $W^{(j)}(T)$  depends on the control as shown in (10). Here the objective function  $\bar{g}(\cdot)$  is the objective  
 function in (5) augmented with a small regularization,

$$\bar{g}(W^{(1)}(T), \dots, W^{(L)}(T)) = \frac{1}{L} \sum_{j=1}^L (\min(W^{(j)}(T) - W^*, 0))^2 + \frac{\lambda}{L} \sum_{j=1}^L W^{(j)}(T)$$

224 with  $\lambda > 0$  a small constant, e.g.,  $\lambda = 10^{-6}$ . The regularization is introduced to resolve the ambiguity of the  
 225 objective function by forcing investment of surplus cash into the risk-free asset.

226 Unfortunately, the stochastic optimization problem (12) solves for the controls at the rebalancing time  
 227 along each path. It has  $O(MNL)$  variables, along with  $O(MNL)$  equality and inequality constraints, which  
 228 becomes computationally challenging to solve in practice since  $L$  is typically very large. Furthermore, the  
 229 solution only provides the control values  $\vec{p}(F^{(j)}(t_0)), \dots, \vec{p}(F^{(j)}(t_{N-1}))$  along each path. It does not immedi-  
 230 ately supply controls at different paths.

231 Given a finite set of sample paths, approximations are necessary to computationally solve this multi-  
 232 stage optimization problems. Finding a good approximation model for the control, suitable for effective  
 233 learning, is the key for computing a solution efficiently and accurately. In the RL or DP approaches, a  
 234 recursive procedure is followed based on dynamic programming principle to simplify the computation of  
 235 the optimal control. We propose to directly solve a global scenario optimization Problem (12) by deploying  
 236 a novel approximation model  $\vec{p}(F(t))$ , using a neural network to represent controls at any time  $t$ ,  $0 \leq t \leq T$ ,  
 237 and any feature state  $F(t)$ .

238 In the proposed approximate model structure, the control is a function of the feature vector which has  
 239 time to go  $T - t$  as a variate. Specifically, let  $F(t_n) \in \mathfrak{R}^d$  denote values of feature variables at  $t_n$ . In the simplest  
 240 case, the feature vector variables can be the wealth at  $t_n$  and time to go, i.e.,  $F(t_n) = \{W(t_n), T - t_n\}$ . More  
 241 generally, the feature variables can include additional market information, e.g., market implied volatility  
 242 or historical realized volatilities. Additionally features can include individual investor's information, e.g.,  
 243 taxes, which personalizes the allocation solution. We note that neural networks have been used to represent  
 244 policies and/or value functions in RL/DP, see, e.g., (Vinyals et al., 2017).

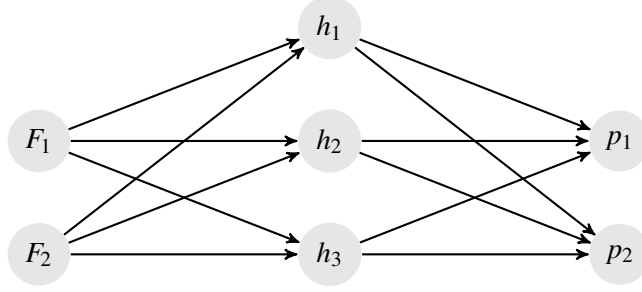


FIGURE 1: A 2-layer NN representing control functions

245 Specifically, we represent the control  $\vec{p}(F(t))$ , for any  $t$ , as the output of an NN and feature  $F(t)$  as  
 246 inputs. At the rebalance time  $t_n$ , the state variable  $F(t_n)$  includes minimally the current wealth  $W(t_n)$  and  
 247 time-to-target-horizon  $T - t_n$ . Thus, in the training, the single NN model outputs the control  $\vec{p}(F(t_n))$  at  $t_n$ ,  
 248  $n = 0, \dots, N-1$ , for any feature state  $F(t_n)$ . In particular, we consider a parsimonious two layer NN, depicted  
 249 in Figure 1, to represent the control function. We remark that shallow learning is also found to outperform  
 250 deep learning for asset pricing in (Gu et al., 2018). We also note that good results are obtained in (Hejazi  
 251 and Jackson, 2016) with an NN containing only one hidden layer (shallow learning). Suppose that input  
 252 features  $F(t) \in \mathfrak{R}^d$  and there are a total of  $M$  assets. Assume that there are  $l$  nodes in the hidden layer of  
 253 NN. This NN is represented by the weights for the input layer and the weights for the output layer.

Assume that  $h \in \mathfrak{R}^l$  is the output of the hidden layer. Let the matrix  $z \in \mathfrak{R}^{dl}$  be the weights from the  
 inputs  $F(t_n) \in \mathfrak{R}^d$  to the hidden nodes  $h \in \mathfrak{R}^l$ . Using the sigmoid activation function,

$$\sigma(u) = \frac{1}{1 + e^u}$$

254 we have

$$h_j(F(t_n)) = \sigma(F_i(t_n) z_{ij}), \quad (13)$$

255 where here (and in the following) we use the summation convention, i.e. summation over repeated indices  
 256 is implied. For example

$$F_i z_{ij} \equiv \sum_{i=1}^{i=d} F_i z_{ij}, \quad j = 1, \dots, l,$$

257 where  $F_i$  is the  $i^{\text{th}}$  component of the feature vector  $F$ .

258 At the output layer, we use the logistic sigmoid. Let the matrix  $x \in \mathfrak{R}^{lM}$  be the weights for the output  
 259 layer. For the  $m^{\text{th}}$  asset,  $1 \leq m \leq M$ , the holding is given by the  $m^{\text{th}}$  component of the output  $\vec{p}$ , i.e.,

$$\vec{p}_m(F(t_n)) = \frac{e^{x_{\ell m} h_{\ell}(F(t_n))}}{\sum_i e^{x_{\ell i} h_{\ell}(F(t_n))}}, \quad 1 \leq m \leq M. \quad (14)$$

Using this representation, the controls automatically satisfy

$$0 \leq \vec{p}(F(t_n)) \leq 1, \quad \vec{p}(F(t_n))^T \mathbf{1} = 1.$$

260 If there are more stringent upper bounds on the assets, they can be similarly incorporated into the represen-  
 261 tation through appropriate scalings.



262 Let  $F^{(j)}(t_n)$  be the state variables at  $t = t_n$  along sample path  $j$ ,  $j \in \{1, \dots, L\}$ . The approximation to the  
 263 optimal learning problem (12) becomes

$$\begin{aligned} & \min_{z \in \mathbb{R}^{dl}, x \in \mathbb{R}^{lM}} \frac{1}{2} \bar{g}(W^{(1)}(T), \dots, W^{(L)}(T)) \\ \text{subject to} \quad & \vec{p}_m(F^{(j)}(t_n)) = \frac{e^{x_{\ell m} h_{\ell}(F^{(j)}(t_n))}}{\sum_i e^{x_{\ell i} h_{\ell}(F^{(j)}(t_n))}}, \quad m = 1, \dots, M, j = 1, \dots, L, n = 0, \dots, N-1 \quad (15) \\ & h_{\ell}(F^{(j)}(t_n)) = \sigma(F_i^{(j)}(t_n) z_{i\ell}), \quad \ell = 1, \dots, l, j = 1, \dots, L, n = 0, \dots, N-1, \end{aligned}$$

264 where we remind the reader that again we use the summation convention. We note that, in the proposed ap-  
 265 proximation model, the constraints in (15) are explicitly satisfied, further simplifying (5) to an unconstrained  
 266 problem (15).

267 In contrast to the large and constrained problem (12), with a dimension of  $O(MNL)$  and  $O(MNL)$  con-  
 268 straints, we note that (15) is an unconstrained optimization problem with  $l(d+M)$  variables, the entries of the  
 269 weight matrices  $z$  and  $x$ . Consequently the dimension of the unconstrained learning optimization problem  
 270 no longer depends on the number of scenarios  $L$  or the number of time steps  $N$ . Rather it depends only on  
 271 the NN model structure.

Let  $\bar{W}(T)$  be the column scenario wealth vector below

$$\bar{W}(T) = [W^{(1)}(T), \dots, W^{(L)}(T)]' .$$

272 Using unconstrained smooth optimization methods to solve (15) requires evaluation of the objective  
 273 function and its derivative with respect to  $z$  and  $x$ . Following (10), each objective function evaluation costs  
 274  $O(l(d+M)NL)$ , or  $O(L)$  assuming a fixed NN model structure and fixed rebalancing schedule.

For the gradient evaluation, we note that

$$\nabla_{x,z} \bar{g} = (\nabla_{\bar{W}} \bar{g}) (\nabla_{x,z} \bar{W}(T))$$

275 where here the gradient  $\nabla_{x,z}$  is with respect to the weight  $x$  and  $z$ .

276 Following (10), we have the iterative computation below for the Jacobian matrices  $\nabla_{x,z} \bar{W}(T)$ ,

$$\begin{aligned} \nabla_{x,z} \bar{W}(t_{n+1}^-) &= \nabla_{x,z} \left( \sum_m R_m(t_n) \vec{p}_m(F(t_n)) (\bar{W}(t_n^-) + q(t_n)) \right) \\ &= \left( \sum_m \vec{R}_m(t_n) \nabla_{x,z} \vec{p}_m(F(t_n)) \right) (\bar{W}(t_n^-) + q(t_n)) + \left( \sum_m \vec{R}_m(t_n) \vec{p}_m(F(t_n)) \right) \nabla_{x,z} W(t_n^-) \end{aligned}$$

and

$$\nabla_{x,z} \bar{W}(t_0^-) = \left( \sum_m R_m(t_0) \nabla_{x,z} \vec{p}_m(F(t_0)) \right) (\bar{W}(t_0^-) + q(t_0))$$

277 Further simplifying notations by dropping dependence on the feature  $F(t_n)$ , the gradient of the control  $\vec{p}$   
 278 is given below, for  $1 \leq q \leq l$ ,  $1 \leq m \leq M$ ,

$$\begin{aligned} \nabla_{x_{qm}} \vec{p}_m &= \overbrace{(1 - \vec{p}_m) \vec{p}_m}^{\text{no sum}} h_q \\ \nabla_{x_{jq}} \vec{p}_m &= -\vec{p}_m \sum_k \frac{e^{x_{\ell j} h_{\ell}}}{e^{x_{\ell k} h_{\ell}}} h_q = -\vec{p}_m \vec{p}_j h_q, \quad j \neq m . \end{aligned}$$

279 Using the definition of the sigmoid function, we also have that, for  $1 \leq j \leq l$ ,  $1 \leq q \leq d$ ,

$$\begin{aligned}
\nabla_{z_{qj}} \vec{p}_m &= \frac{e^{x_{\ell m} h_{\ell}}}{\sum_k e^{x_{\ell k} h_{\ell}}} \left( x_{jm} - \frac{\sum_{k=1}^M e^{x_{\ell k} h_{\ell}} x_{jk}}{\sum_{k=1}^M e^{x_{\ell k} h_{\ell}}} \right) \overbrace{\nabla_{z_{qj}} \cdot}^{no\ sum} \vec{h}_j \\
&= -\vec{p}_m \left( x_{jm} - \frac{\sum_{k=1}^M e^{x_{\ell k} h_{\ell}} x_{jk}}{\sum_k e^{x_{\ell k} h_{\ell}}} \right) \frac{e^{F_{\ell} z_{\ell j}}}{(1 + e^{F_{\ell} z_{\ell j}})^2} F_q.
\end{aligned}$$

280 The gradient evaluation costs  $O(l(d+M)NL)$ , and the Hessian computation costs  $O(l^2(d+M)^2LN)$ , using  
281 a finite difference of the gradient. Given the function/gradient/Hessian, solving the trust region subproblem  
282 requires  $O((l(d+M))^3)$ . Since the dimension of the optimization problem  $l(d+M)$  is small for the problem  
283 considered in this paper, e.g.,  $l(d+M) = 15$  for three assets, function/gradient/Hessian evaluations become  
284 the dominant cost and the usage of a trust region subproblem is a reasonable computational choice.

## 285 5 Ground truth: a low dimensional parametric return model

286 Given a parametric model of the underlying stochastic process, for a small number of random factors, we  
287 can solve (15) by computing the solution of the associated Hamilton Jacobi Bellman (HJB) equation (Dang  
288 and Forsyth, 2014).

289 We first validate the proposed data driven NN approach (15) for determining the optimal controls for  
290 Problem (5) by comparing the solution to that from solving the HJB equation under a parametric model,  
291 assuming a portfolio with two assets. Let  $S(t)$  and  $B(t)$  respectively denote the *amounts* invested in the risky  
292 and risk-free assets at time  $t$ ,  $t \in [0, T]$ . In practice, we will suppose that  $S(t)$  represents the amount invested  
293 in a broad stock market index, while  $B(t)$  is the amount invested in short term default-free government bonds.

294 In general, the amounts  $S(t)$  and  $B(t)$  will depend on the investor's strategy over time, including contri-  
295 butions, withdrawals, and portfolio rebalances, as well as changes in the unit prices of the assets. Suppose  
296 for the moment that the investor does not take any action with respect to the controllable factors. We refer  
297 to this as the absence of control. This situation applies in between the rebalancing times. In this case, we  
298 assume that  $S(t)$  follows a jump diffusion process. Recall that  $t^- = t - \epsilon$ ,  $\epsilon \rightarrow 0^+$ , i.e.  $t^-$  is the instant of time  
299 before  $t$ , and let  $\xi$  be a random number representing a jump multiplier. When a jump occurs,  $S(t) = \xi S(t^-)$ .  
300 Allowing discontinuous jumps lets us explore the effects of severe market crashes on the risky asset holding.  
301 We assume that  $\xi$  follows a double exponential distribution (Kou, 2002; Kou and Wang, 2004). If a jump  
302 occurs,  $p_{up}$  is the probability of an upward jump, while  $1 - p_{up}$  is the chance of a downward jump. The  
303 density function for  $y = \log \xi$  is

$$f(y) = p_{up} \eta_1 e^{-\eta_1 y} \mathbf{1}_{y \geq 0} + (1 - p_{up}) \eta_2 e^{\eta_2 y} \mathbf{1}_{y < 0}. \quad (16)$$

304 For future reference, note that

$$E[y = \log \xi] = \frac{p_{up}}{\eta_1} - \frac{(1 - p_{up})}{\eta_2}, \quad E[\xi] = \frac{p_{up} \eta_1}{\eta_1 - 1} + \frac{(1 - p_{up}) \eta_2}{\eta_2 + 1}. \quad (17)$$

305 In the absence of control,  $S(t)$  evolves according to

$$\frac{dS(t)}{S(t^-)} = (\mu - \lambda E[\xi - 1]) dt + \sigma dZ + d \left( \sum_{i=1}^{\pi_t} (\xi_i - 1) \right), \quad (18)$$

306 where  $\mu$  is the (uncompensated) drift rate,  $\sigma$  is the volatility,  $dZ$  is the increment of a Wiener process,  $\pi_t$   
307 is a Poisson process with positive intensity parameter  $\lambda$ , and  $\xi_i$  are i.i.d. positive random variables having  
308 distribution (16). Moreover,  $\xi_i$ ,  $\pi_t$ , and  $Z$  are assumed to all be mutually independent.

$\mu$	$\sigma$	$\lambda$	$p_{up}$	$\eta_1$	$\eta_2$
Real CRSP Cap-Weighted Index					
.08889	.14771	.32222	0.27586	4.4273	5.2613
Real CRSP Equal-Weighted Index					
.11833	.16633	.40000	.33334	3.6912	4.5409

TABLE 1: *Estimated annualized parameters for double exponential jump diffusion model. Cap-weighted and equal-weighted CRSP indexes, deflated by the CPI. Sample period 1926:1 to 2015:12.*

309 In the absence of control, we assume that the dynamics of the amount  $B_t$  invested in the risk-free asset  
310 are

$$dB(t) = rB(t) dt, \quad (19)$$

311 where  $r$  is the (constant) risk-free rate. This is obviously a simplification of the real bond market. We remind  
312 the reader that, ultimately, our NN method is entirely data driven, and will be based on bootstrapped stock  
313 and bond indexes.

314 With this parametric model of stock prices, we can determine the optimal solution to Problem (5) using  
315 dynamic programming. This in turn results in a nonlinear Hamilton-Jacobi-Bellman PDE. We use the meth-  
316 ods described in (Dang and Forsyth, 2014; Forsyth and Labahn, 2018) to determine the provably optimal  
317 solution (to within a tolerance). At each rebalancing date  $t_n$ , at each value of  $W(t_n^-)$ , we check to see if  
318 equation (7) holds, which indicates that surplus cash is available. In this case we withdraw the surplus cash  
319 from the portfolio, and invest the remainder in the risk-free asset. We also invest the surplus cash in the  
320 risk-free asset. This is an optimal strategy, as described in Dang and Forsyth (2016).

## 321 6 Data

322 Our data is from the Center for Research in Security Prices (CRSP) on a monthly basis over the 1926:1-  
323 2015:12 period.<sup>1</sup> Our base case tests use the CRSP 3-month Treasury bill (T-bill) index for the risk-free asset  
324 and the CRSP cap-weighted total return index for the risky asset. This latter index includes all distributions  
325 for all domestic stocks trading on major U.S. exchanges. As an alternative case for additional illustrations,  
326 we replace the above two indexes by a 10-year Treasury index and the CRSP equal-weighted total return  
327 index.<sup>2</sup> All of these various indexes are in nominal terms, so we adjust them for inflation by using the  
328 U.S. CPI index, also supplied by CRSP. We use real indexes since investors saving for retirement should be  
329 focused on real (not nominal) wealth goals.

330 In the case of the parametric model, i.e., processes (18) and (19), we use the methods in Dang and  
331 Forsyth (2016) to calibrate the process parameters. We use a threshold technique (Cont and Mancini, 2011)  
332 to identify jump frequency and distribution, and the methods in (Dang and Forsyth, 2016) to determine  
333 the remaining parameters. Annualized estimated parameters for both the cap-weighted and equal-weighted  
334 indexes are provided in Table 1.

<sup>1</sup>More specifically, results presented here were calculated based on data from Historical Indexes, ©2015 Center for Research in Security Prices (CRSP), The University of Chicago Booth School of Business. Wharton Research Data Services was used in preparing this article. This service and the data available thereon constitute valuable intellectual property and trade secrets of WRDS and/or its third-party suppliers.

<sup>2</sup>The 10-year Treasury index was constructed from monthly returns from CRSP back to 1941. The data for 1926-1941 were interpolated from annual returns in Homer and Sylla (2005).

	Real 3-month T-bill Index	Real 10-year Treasury Index
Mean return	.00827	.02160
Volatility	.019	.065

TABLE 2: Mean annualized real rates of return for bond indexes ( $\log[B(T)/B(0)]/T$ ). Volatilities (annualized) computed using log returns. We show the volatilities for information only, the parametric model uses a constant average real interest rate. Sample period 1926:1 to 2015:12.

335 Table 2 shows the average real interest rates for the 3-month T-bill and 10-year U.S. Treasury indexes  
336 over the entire sample period from 1926 to 2015.

## 337 7 Bootstrap resampling

338 In order to use the proposed data driven NN approach, we will sample directly from the historical data.  
339 A single bootstrap resampled path is constructed as follows. Suppose the investment horizon is  $T$  years.  
340 We divide this total time into  $k$  blocks of size  $b$  years, so that  $T = kb$ . We then select  $k$  blocks at random  
341 (with replacement) from the historical data (from both the deflated stock and bond indexes). Each block  
342 starts at a random month. We then form a single path by concatenating these blocks. Since we sample  
343 with replacement, the blocks can overlap. To avoid end effects, the historical data is wrapped around, as  
344 in the circular block bootstrap (Politis and White, 2004; Patton et al., 2009). We repeat this procedure for  
345 many paths. The sampling is done in blocks in order to account for possible serial dependence effects in the  
346 historical time series. The choice of blocksize is crucial and can have a large impact on the results (Cogneau  
347 and Zakalmouline, 2013). We simultaneously sample the real stock and bond returns from the historical  
348 data. This introduces random real interest rates in our samples, in contrast to the constant interest rates  
349 assumed in the synthetic market tests and in the determination of the optimal controls.

350 To reduce the impact of a fixed blocksize and to mitigate the edge effects at each block end, we use the  
351 stationary block bootstrap (Politis and White, 2004; Patton et al., 2009). The blocksize is randomly sampled  
352 from a geometric distribution with an expected blocksize  $\hat{b}$ . The optimal choice for  $\hat{b}$  is determined using  
353 the algorithm described in Patton et al. (2009). This approach has also been used in other tests of portfolio  
354 allocation problems recently (e.g. Dichtl et al., 2016). Calculated optimal values for  $\hat{b}$  for the various indexes  
355 are given in Table 3.

356 When we use our resampling method in the proposed data driven NN approach, we will simultaneously  
357 sample the same block from all data sets (i.e. equity indices and bond indices). Clearly, Table 3 shows that  
358 the optimal blocksize varies amongst the time series in question. It is, therefore, not clear which is the best  
359 choice of blocksize for use in our simultaneous resampling method. As a result, we will carry out tests with  
360 a variety of blocksizes, in the ranges suggested by Table 3.

## 361 8 Numerical Results: Parametric Model

362 In this section, we give results based on the parametric model described in Section 5. Optimal controls will  
363 be computed using both the HJB equation method and the data driven NN technique (15). All examples will  
364 assume the scenario given in Table 4.

Data series	Optimal expected block size $\hat{b}$ (months)
Real 3-month T-bill index	50.1
Real 10-year Treasury index	4.7
Real CRSP cap-weighted index	1.8
Real CRSP equal-weighted index	10.4

TABLE 3: Optimal expected blocksize  $\hat{b} = 1/v$  when the blocksize follows a geometric distribution  $Pr(b = k) = (1-v)^{k-1}v$ . The algorithm in Patton et al. (2009) is used to determine  $\hat{b}$ .

	Base Case	Alternative Case
Investment horizon (years)	30	30
Equity market index	Cap-weighted	Equal-weighted
Risk-free asset index	3-month T-bill	10-year Treasury
Initial investment $W_0$ (\$)	0.0	0.0
Real investment each year (\$)	10.0	10.0
Rebalancing interval (years)	1	1

TABLE 4: Input data for examples. Cash is invested at  $t = 0, 1, \dots, 29$  years. Market parameters are provided in Tables 1 and 2

## 365 8.1 Optimal control: HJB equation

366 The optimal control is computed by solving an HJB equation as described in Dang and Forsyth (2014);  
367 Forsyth and Labahn (2018).

### 368 8.1.1 HJB equation, base case: CRSP value weighted index and 3-month T-bill

369 As a first example, we consider the base case input data summarized in Table 4. An investor with a horizon of  
370 30 years makes real contributions each year of \$10, allocated between the CRSP cap-weighted and 3-month  
371 T-bill indexes and rebalanced annually.

372 We first use a constant proportion strategy, where we rebalance to a fixed weight in stocks at each  
373 rebalancing date ( $p = 0.5$ ), and determine the expected value of the terminal real wealth for this strategy. We  
374 then use this expected value as a constraint and determine the optimal strategy which solves problem (5). In  
375 other words, the value of  $W^*$  in the objective function of (5) is determined by setting  $\mathbf{E}(W_T)$  to be the same  
376 as for the constant weight strategy. We compute and store the optimal strategy (from the HJB solution).

377 We evaluate the performance of the various strategies using Monte Carlo simulation, where we simulate  
378 the market using the SDEs in equations (18-19). We use the constant weight strategy and the optimal  
379 strategy determined from the HJB solution. Table 5 compares the results for these strategies. Due to the  
380 highly skewed distribution function for the final wealth  $W_T$ , the most relevant statistics are the median and  
381 the probability of shortfall. Both of these statistics are highly favourable for the optimal strategy.

### 382 8.1.2 HJB equation: alternative case, CRSP equal-weighted index and 10-year Treasury index

383 To provide a second example for the parametric model, we use alternative assets. In particular, as indicated  
384 in Table 4, we replace the CRSP cap-weighted index with its equal-weighted counterpart, and we substitute

Strategy	$E[W_T]$	Median $[W_T]$	std $[W_T]$	Probability of Shortfall	
				$W_T < 500$	$W_T < 600$
Constant proportion ( $p = 0.5$ )	705	630	350	.28	.45
Optimal	705	775	153	.12	.17

TABLE 5: Parametric model results from 160,000 Monte Carlo simulation runs for base case input data given in Table 4 and corresponding parameters from Tables 1 (threshold) and 2. The expected surplus cash flow for the optimal adaptive strategy is 16.7, assumed to be invested in the risk-free asset.

Strategy	$E[W_T]$	Median $[W_T]$	std $[W_T]$	Probability of Shortfall	
				$W_T < 700$	$W_T < 900$
Constant proportion ( $p = 0.5$ )	1082	875	852	.33	.52
Optimal	1082	1238	338	.17	.23

TABLE 6: Parametric model results from 160,000 Monte Carlo simulation runs for alternative case input data given in Table 4 and corresponding parameters from Tables 1 (threshold) and 2. The expected surplus cash flow for the optimal adaptive strategy is 51, assumed to be invested in the risk-free asset.

385 the 10-year Treasury bond index for the 3-month Treasury bill index. See Tables 1 and 2 for relevant corre-  
386 sponding parameter estimates. We retain the same assumptions regarding investment horizon, rebalancing  
387 frequency, and real cash contributions as for the base case Table 4.

388 Table 6 presents the results for the constant proportion, and optimal adaptive strategies. The results are  
389 very similar in qualitative terms to those seen earlier for the base case in Table 4, though investing in these  
390 two assets leads to a terminal wealth distribution with a higher mean and standard deviation relative to using  
391 the cap-weighted index and 3-month T-bills. Note that the median of  $W_T$  is higher than the mean for the  
392 optimal strategy, and the probabilities of shortfall are much reduced compared with the constant proportion  
393 strategy.

## 394 8.2 Optimal NN controls

395 We compute the approximate optimal control by solving the proposed NN approximation (15) to the original  
396 problem (5), as described in Section 4. Specifically, we have found that a parsimonious NN model with one  
397 hidden layer of three nodes is sufficient to produce nearly optimal performance. In this investigation, the  
398 feature vector consists of simply the current wealth and time-to-go. We explicitly compute the objective  
399 function and its first order derivatives but approximate the Hessian matrix using a finite difference approxi-  
400 mation. The NN approximation problem (15) is solved using a trust region method (Coleman and Li, 1996).  
401 For the NN learning, it is known that standardizing features is important for efficient learning. For (15),  
402 however, the feature state, wealth  $W(t_n)$ , changes with the control iterate during the optimization process.  
403 Hence we cannot standardize features based on standard deviations of wealth values of the current iteration.  
404 Instead, at each rebalance time  $t_n$ ,  $n = 1, \dots, N - 1$ , we use standard deviations associated with the constant  
405 proportion strategy to scale the wealth feature variable.

## 406 8.3 Base case NN controls: CRSP cap-weighted index and 3-month T-bill

407 We generate  $L = 160,000$  i.i.d. random return paths for the parametric jump model calibrated from the his-  
408 toric market data, as described in §5, using equations (18) and (19). We solve the NN learning optimization

Training Error on Synthetic Data : Market Cap Weighted					
Strategy	$E(W_T)$	$std(W_T)$	$median(W_T)$	$Pr(W_T < 500)$	$Pr(W_T < 600)$
constant proportion ( $p = .5$ )	705	350	630	0.28	0.45
NN adaptive	705	159	782	0.13	0.18
Optimal	705	153	782	0.12	0.17

TABLE 7: Training comparison base case data, Table 4. Value weighted CRSP and 3 month T-bill. Training carried out using 160,000 sampled paths. Compare with Table 5.

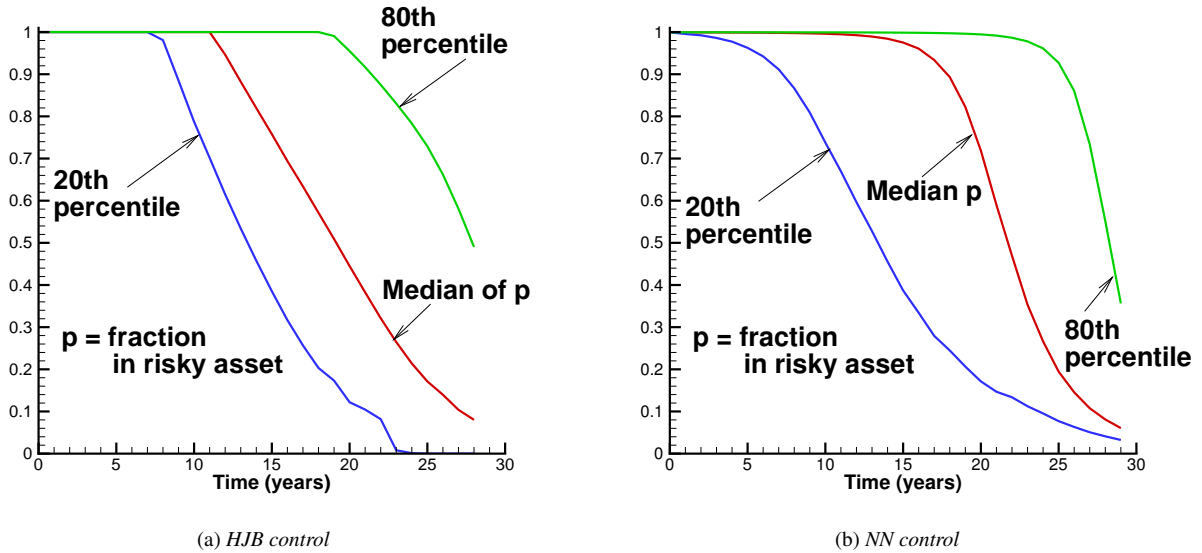


FIGURE 2: Percentiles of the control (fraction in equity index), NN and HJB equation solution, base case example, Table 4 (cap-weighted CRSP index and 3-month T-bill).

409 problem (15).

410 Table 7 presents training performance comparisons of the optimal controls obtained for the cap-weighted  
411 index and 3-month T-bill two asset base case. Comparing to the performance of the optimal controls com-  
412 puted by solving HJB equation in Tables 5, we observe that the proposed NN approach (15) achieves excel-  
413 lent performance using a parsimonious NN model with  $d = 2$ ,  $l = 3$ ,  $M = 2$  for the 2-asset case, totaling only  
414 12 parameters for  $z$  and  $x$ . Considering that there is always error due to sampling, the slight suboptimality  
415 arising from the NN approximation seems to be quite acceptable.

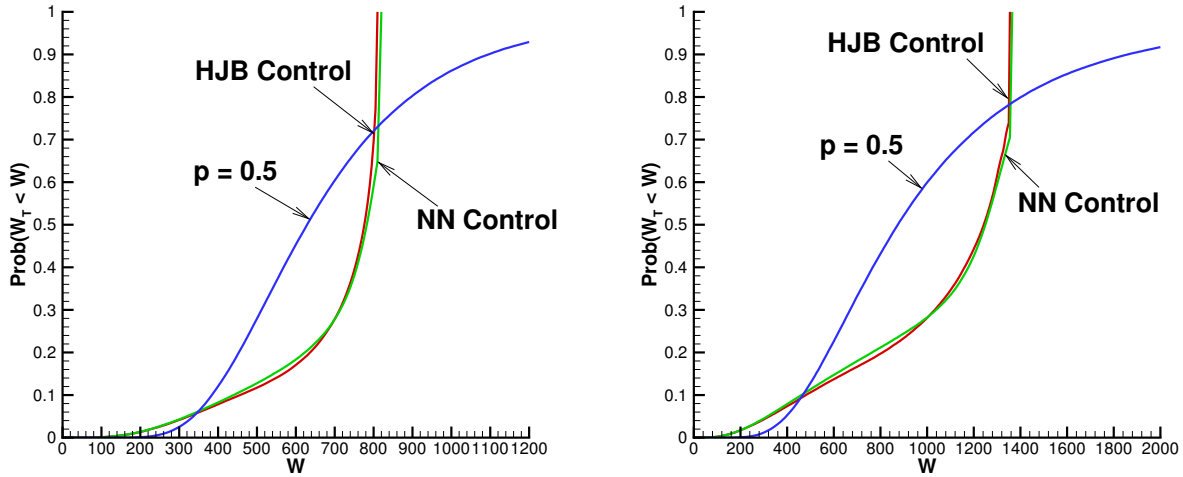
416 Corresponding to the base case, Table 4, Figure 2 compares the percentiles of the NN controls with  
417 those computed using the HJB equation. We observe that the curves from the NN and HJB controls are  
418 qualitatively similar, indicating similar investment strategies are obtained.

#### 419 8.4 Alternative case NN controls: CRSP equal-weighted index and 10-year Treasury index

420 We also compare the NN controls for the alternative case, CRSP equal-weighted index and 10-year treasury  
421 index, in Table 8. Again, it is remarkable that our parsimonious NN model, trained on sampled data, is able  
422 to get very close to the optimal results.

Training Error on Synthetic Data: Equal Weighted					
Strategy	$E(W_T)$	$std(W_T)$	$median(W_T)$	$Pr(W_T < 700)$	$Pr(W_T < 900)$
constant proportion ( $p = .5$ )	1082	852	875	0.33	0.52
NN adaptive	1082	349	1250	0.18	0.24
Optimal	1082	338	1238	0.17	0.23

TABLE 8: Training comparison alternative case data, Table 4. Equal weighted CRSP and 10 year treasury. Training carried out using 160000 sampled paths. Compare with Table 6.



(a) Cap-weighted CRSP, 3 month T-bill.

(b) Equal-weighted CRSP, 10 year Treasury.

FIGURE 3: Comparison of the cumulative distribution functions for the control computed using HJB equation and Neural Network (NN). 160,000 MC samples used. The constant weight strategy ( $p = 0.5$ ) also shown. Base case (Figure 3(a)) and alternative case (Figure 3(b)) data sets, as in Table 4.  $W^* = 806$  (base case) and  $W^* = 1355$  (alternative case). Surplus cash is not included in the distribution functions for the HJB and NN controls.

## 423 8.5 Comparison of Cumulative Distribution Functions: Parametric Market Model

424 Figure 3 shows the cumulative distribution functions, computed using 160,000 Monte Carlo simulations,  
 425 for both the base case assets and the alternative case. The controls were computed by (i) solving the HJB  
 426 equation (which gives the optimal strategy), (ii) using the NN approximation and (iii) using the constant  
 427 weight strategy  $p = 0.5$ , i.e., rebalance to a fraction of 0.5 in equities at each rebalancing date.

428 Figure 3 shows that the control computed using a very parsimonious NN model can reproduce very  
 429 closely the entire distribution function of the terminal wealth generated using the optimal HJB equation  
 430 control.

## 431 8.6 Test performance of the NN control in the historic market scenarios

432 We compute and store the NN strategy, based on sampled data, which is generated using the parametric  
 433 model described by equations (18) and (19). We then test this learned control on the bootstrapped historical  
 434 market data.

435 Tables 9 and 10 report test performance of the strategies computed using the simulated returns and  
 436 present their performance on on the bootstrapped resampled historical data. We show the results obtained



Test Error: Market Cap Weighted					
Strategy	$E(W_T)$	$std(W_T)$	$median(W_T)$	$Pr(W_T) < 500$	$Pr(W_T < 600)$
Expected Blocksize $\hat{b} = 0.5$ years					
constant proportion ( $p = .5$ )	680	278	627	0.28	0.46
NN adaptive	699	154	766	0.12	0.19
Expected Blocksize $\hat{b} = 1$ years					
constant proportion ( $p = .5$ )	680	277	626	0.28	0.45
NN adaptive	698	154	765	0.13	0.19
Expected Blocksize $\hat{b} = 2$ years					
constant proportion ( $p = .5$ )	677	264	628	0.27	0.46
NN adaptive	704	144	764	0.11	0.18
Expected Blocksize $\hat{b} = 5$ years					
constant proportion ( $p = .5$ )	675	250	635	0.27	0.44
NN adaptive	713	136	776	0.10	0.16
Expected Blocksize $\hat{b} = 8$ years					
constant proportion ( $p = .5$ )	666	231	631	0.26	0.44
NN adaptive	718	127	777	0.08	0.15
Expected Blocksize $\hat{b} = 10$ years					
constant proportion ( $p = .5$ )	667	223	634	0.25	0.44
NN adaptive	721	123	779	0.08	0.14

TABLE 9: NN control computed and stored based on sampling the parametric market model. Tests carried out using 10000 bootstrap resamples of historical data. Cap-weighted CRSP index and 3-month T-bill market data. Compare to the training performance in Table 7.

437 by rebalancing to a constant equity weight  $p = 0.5$ . Since the optimal choice of blocksize is not clear (being  
438 quite different for the stock index and the bond index) we show results for a range of reasonable blocksizes.  
439 Comparing the result in Tables 9 and 10 to the results in Tables 7 & 8 respectively, we observe that the  
440 test performance comparisons with the constant proportion strategies are similar to the training performance  
441 comparisons, suggesting robustness of the NN control. In particular, in all cases, the NN control (trained  
442 using the parametric model) has a higher  $Median(W_T)$  and smaller probabilities of shortfall, compared to  
443 the constant weight strategy.

## 444 8.7 Performance of the optimal controls directly learned from historic market data

445 We now abandon the parametric market model, and operate directly on the historical market data. Since we  
446 have no *optimal* solution for this case, we contrast performance from the NN control with the performance  
447 from the constant weight strategy, rebalancing to a constant weight  $p = 0.5$  in equities at each rebalancing  
448 date.

449 We emphasize that a key advantage of the proposed optimal NN control framework is that it allows  
450 direct learning of the controls from the market data, bypassing the parametric modeling all together. In §8.3,  
451 we have seen that the performance of the optimal NN controls, trained from samples determined from the  
452 parametric market model, is comparable to that from the optimal HJB controls.

453 Furthermore, in §8.6, the performance of the NN control (trained from parametric model samples) using  
454 the bootstrapped historical market data is shown to be robust. Here we report the training performance of  
455 the optimal NN controls directly from the market data. As an additional robustness check, we compute and  
456 store the NN controls trained on resampled historical market data, and then test the performance of these  
457 learned controls on samples from the parametric market model.

458 Table 11 presents training performance comparisons of the NN controls directly learned from the histor-  
459 ical cap-weighted index and 3-month T-bill market data. A range of blocksizes for the bootstrap resampling  
460 is reported. For each blocksize, we determine  $W^*$  such that  $E[W_T]$  for the NN control is the same as  $E[W_T]$   
461 for the constant proportion strategy. The NN controls for each blocksize are stored, and then used as controls

Test Error: Market Equal Weighted					
Strategy	$E(W_T)$	$std(W_T)$	$median(W_T)$	$Pr(W_T) < 700$	$Pr(W_T < 900)$
Expected Blocksize $\hat{b} = 0.5$ years					
constant proportion ( $p = .5$ )	1005	586	868	0.33	0.53
NN adaptive	1057	331	1177	0.18	0.26
Expected Blocksize $\hat{b} = 1$ years					
constant proportion ( $p = .5$ )	1005	586	868	0.33	0.53
NN adaptive	1057	331	1177	0.18	0.26
Expected Blocksize $\hat{b} = 2$ years					
constant proportion ( $p = .5$ )	961	465	865	0.31	0.54
NN adaptive	1082	293	1167	0.13	0.22
Expected Blocksize $\hat{b} = 5$ years					
constant proportion ( $p = .5$ )	936	382	869	0.29	0.54
NN adaptive	1111	261	1182	0.10	0.18
Expected Blocksize $\hat{b} = 8$ years					
constant proportion ( $p = .5$ )	921	346	867	0.28	0.54
NN adaptive	1124	243	1185	0.08	0.16
Expected Blocksize $\hat{b} = 10$ years					
constant proportion ( $p = .5$ )	919	336	870	0.27	0.54
NN adaptive	1132	233	1190	0.07	0.16

TABLE 10: NN control computed and stored based on sampling the parametric market model. Tests carried out using 10000 bootstrap resamples of historical data. Equal-weighted CRSP index and 10 year treasury market data. Compare to the training performance in Table 7.

462 for Monte Carlo simulations based on the parametric market model. Table 12 reports the results of these  
463 tests. Comparing these tables to Table 7 and 9 respectively, we note a striking similarity of training and test  
464 performance comparisons. There is some degradation in performance as the blocksize increases, when we  
465 test on the parametric model, but  $median(W_T)$  is always larger for the NN control, compared to the constant  
466 weight strategy. However, this is a good test of robustness of the controls. Small blocksizes simulate an  
467 i.i.d. process, which is the underlying assumption of the parametric market model. Increasing the blocksize  
468 causes a deviation from the i.i.d. assumption, and hence is stress test for the control learned with a large  
469 blocksize.

470 We carry out a similar sequence of tests using the alternative market data, based on an equal-weight  
471 index, and 10 year treasuries. Table 13 presents training performance comparisons of the NN controls  
472 directly learned from the historical equal-weighted index and 10-year treasury market data. Table 14 reports  
473 the test performance of these NN controls, learned from the market data, on the simulated data from the  
474 corresponding parametric market model.

475 Comparing Tables 13 and 14 to Tables 8 and 10 respectively, we note that the same similarity in training  
476 and test performance comparisons. In Table 14, we note that there is some degradation in performance, in  
477 terms of  $E(W_T)$  as the blocksize is increased, but, as discussed previously, this can be traced to the fact that  
478 use of large blocksizes causes departures from the i.i.d. process assumed in the parametric model. In any  
479 case, the important statistic here is  $median(W_T)$ , which is always larger for the NN control compared to the  
480 constant weight strategy. However, once again, the NN control is quite robust. Of course, this suggests  
481 that if we believe that the true market process is better modeled as i.i.d., then use of smaller blocksizes will  
482 obviously yield superior results.

## 483 8.8 Three assets

484 In addition to the clear advantage of learning the strategy directly from market data, and avoiding the need  
485 to specify and calibrate a parametric market mode, we can, with trivial modification, use the NN approach  
486 to solve high dimensional asset allocation problems. Recall that the overall complexity of the proposed NN

Training Error: Market Cap Weighted					
Strategy	$E(W_T)$	$std(W_T)$	$median(W_T)$	$Pr(W_T < 500)$	$Pr(W_T < 600)$
Expected Blocksize $\hat{b} = 0.5$ years					
constant proportion ( $p = .5$ )	680	278	627	0.28	0.46
NN adaptive	680	142	764	0.13	0.20
Expected Blocksize $\hat{b} = 1$ years					
constant proportion ( $p = .5$ )	680	277	626	0.28	0.45
NN adaptive	680	142	762	0.13	0.20
Expected Blocksize $\hat{b} = 2$ years					
constant proportion ( $p = .5$ )	677	264	628	0.27	0.46
NN adaptive	677	127	748	0.12	0.19
Expected Blocksize $\hat{b} = 5$ years					
constant proportion ( $p = .5$ )	675	250	635	0.27	0.44
NN adaptive	675	112	731	0.10	0.16
Expected Blocksize $\hat{b} = 8$ years					
constant proportion ( $p = .5$ )	666	231	631	0.26	0.44
NN adaptive	666	97	711	0.08	0.15
Expected Blocksize $\hat{b} = 10$ years					
constant proportion ( $p = .5$ )	667	223	634	0.25	0.44
NN adaptive	667	92	707	0.08	0.14

TABLE 11: Training performance comparisons on the market data: The NN controls are learned directly from the cap-weighted index and 3-month T-bill market data. The expected blocksize is used in the bootstrap resampling algorithm, 10,000 samples used. Bootstrap resampling also used for the  $p = 0.5$  control.

Test Error: Market Cap Weighted						
Strategy	$E(W_T)$	$std(W_T)$	$median(W_T)$	$Pr(W_T < 500)$	$Pr(W_T < 600)$	$\hat{b}$ years
constant proportion ( $p = .5$ )	705	350	630	0.28	0.45	NA
NN adaptive	682	146	765	0.13	0.20	0.5
NN adaptive	679	147	763	0.14	0.21	1.0
NN adaptive	671	141	747	0.13	0.20	2.0
NN adaptive	658	149	740	0.16	0.23	5.0
NN adaptive	643	140	716	0.16	0.22	8.0
NN adaptive	640	138	711	0.16	0.22	10.0

TABLE 12: The NN controls are learned directly from the cap-weighted index and 3-month T-bill market data, using bootstrap resampling, with the expected blocksize  $\hat{b}$  indicated. These controls are then used in Monte Carlo simulations based on the parametric market model.

Training Error: Market Equal Weighted					
Strategy	$E(W_T)$	$std(W_T)$	$median(W_T)$	$Pr(W_T < 700)$	$Pr(W_T < 900)$
Expected Blocksize $\hat{b} = 0.5$ years					
constant proportion ( $p = .5$ )	1005	586	868	0.33	0.53
NN adaptive	1005	289	1205	0.18	0.27
Expected Blocksize $\hat{b} = 1$ years					
constant proportion ( $p = .5$ )	1005	586	868	0.33	0.53
NN adaptive	1005	289	1205	0.18	0.27
Expected Blocksize $\hat{b} = 2$ years					
constant proportion ( $p = .5$ )	961	465	865	0.31	0.54
NN adaptive	961	207	1081	0.13	0.24
Expected Blocksize $\hat{b} = 5$ years					
constant proportion ( $p = .5$ )	936	382	869	0.29	0.54
NN adaptive	936	151	1007	0.09	0.20
Expected Blocksize $\hat{b} = 8$ years					
constant proportion ( $p = .5$ )	921	346	867	0.28	0.54
NN adaptive	921	124	972	0.07	0.18
Expected Blocksize $\hat{b} = 10$ years					
constant proportion ( $p = .5$ )	919	336	870	0.27	0.54
NN adaptive	919	114	964	0.07	0.17

TABLE 13: Training performance comparisons on the market data: The NN controls are learned directly from the equal-weighted CRSP index and 10 year treasury market data. The expected blocksize is used in the bootstrap resampling algorithm, 10,000 samples used. Bootstrap resampling also used for the  $p = 0.5$  control.

Test Error: Market Equal Weighted						
Strategy	$E(W_T)$	$std(W_T)$	$median(W_T)$	$Pr(W_T < 700)$	$Pr(W_T < 900)$	$\hat{b}$ years
constant proportion ( $p = .5$ )	1082	852	875	0.33	0.52	NA
NN adaptive	1011	303	1205	0.18	0.26	0.5
NN adaptive	1011	303	1205	0.18	0.26	1.0
NN adaptive	939	254	1081	0.18	0.25	2.0
NN adaptive	889	226	1007	0.17	0.25	5.0
NN adaptive	865	214	972	0.17	0.24	8.0
NN adaptive	860	212	964	0.17	0.24	10.0

TABLE 14: The NN controls are learned directly from the equal-weighted CRSP index and 10 year treasury market data, using bootstrap resampling, with the expected blocksize  $\hat{b}$  indicated. These controls are then used in Monte Carlo simulations based on the parametric market model.

Training with Expected Blocksize $\hat{b} = 0.5$ years: Market Cap Weighted					
Strategy	$E(W_T)$	$std(W_T)$	$median(W_T)$	$Pr(W_T) < 500$	$Pr(W_T < 600)$
Expected Blocksize $\hat{b} = 0.5$ years					
constant proportion ( $p = (0.6, 0.1, 0.3)$ )	860	450	758	0.18	0.31
NN adaptive	860	264	986	0.15	0.20
Expected Blocksize $\hat{b} = 1$ years					
constant proportion ( $p = (0.6, 0.1, 0.3)$ )	857	429	761	0.18	0.30
NN adaptive	865	264	994	0.15	0.20
Expected Blocksize $\hat{b} = 2$ years					
constant proportion ( $p = (0.6, 0.1, 0.3)$ )	849	414	758	0.18	0.30
NN adaptive	867	254	986	0.13	0.19
Expected Blocksize $\hat{b} = 5$ years					
constant proportion ( $p = (0.6, 0.1, 0.3)$ )	841	383	769	0.17	0.29
NN adaptive	878	246	994	0.12	0.18
Expected Blocksize $\hat{b} = 8$ years					
constant proportion ( $p = (0.6, 0.1, 0.3)$ )	827	350	769	0.16	0.28
NN adaptive	886	236	996	0.11	0.16
Expected Blocksize $\hat{b} = 10$ years					
constant proportion ( $p = (0.6, 0.1, 0.3)$ )	826	337	772	0.16	0.27
NN adaptive	893	230	1002	0.10	0.15

TABLE 15: Performance comparisons using the cap-weighted index, 3-month T-bill and 10-year treasury: the first data set with the expected blocksize  $\hat{b} = 0.5$  years is the training set. Test performance comparisons are reported on the remaining data sets.

control approach is  $O(\max((l(d+M))^3, (l^2(d+M)^2LN))$  where  $d$  is the number of features,  $l$  is the number of nodes,  $M$  is the number of assets, and  $N$  is the number of timesteps.

In this section, we report performance on a three asset portfolio. As a point of comparison, we consider a base case strategy to be a constant proportion strategy, which rebalances to the weights: 60% in the equity index, 10% in the 3-month T-bill, and 30% in the 10-year Treasury. As before, we select  $W^*$  so that  $E[W_T]$  is the same for the NN control and for the constant weight strategy, for the training set. All tests in this section are based on bootstrap historical market simulations.

Table 15 presents performance comparisons using the cap-weighted index, 3-month T-bill and 10-year treasury. The data set with the expected blocksize  $\hat{b} = 0.5$  years is used to train the NN control model and its test performance is reported on the other five data sets with different expected blocksizes. Table 16 reports the same comparisons except that the data set with the expected blocksize  $\hat{b} = 10$  years is used to train the NN control model.

We observe that, in the three-asset case, the training and testing performances of the NN controls continue to dominate that of the constant proportion strategy, achieving a performance enhancement level similar to the two-asset case. In addition, performance comparison is robust. In all cases,  $median(W_T)$  for the NN control is larger than for the constant weight strategy, with reduced probability of shortfall.

Finally, we replace the the cap-weighted index by the CRSP equal-weighted index, but continue with the 3-month T-bill and 10 year treasury for the fixed income components of the portfolio. As before, we compare to a constant proportion strategy with weights 60 : 10 : 30 in the equity index, 3-month T-bill and 10-year treasury. We consider this alternative three-asset case and learn the NN controls from the market data directly. Table 17 presents performance comparisons using these portfolio components. The data set with the expected blocksize  $\hat{b} = 0.5$  years is used to train the NN control model and its test performance is reported on the other five data sets with different expected blocksizes. Table 16 reports the same comparisons except that the data set with the expected blocksize  $\hat{b} = 10$  years is used to train the NN control model. We observe similar performance comparisons as for the cap-weighted index case.

In Figure 4, we compare cumulative distributions of the NN control on the training data ( $\hat{b} = .5$ ) and testing data ( $\hat{b} = 10$ ) and compare them to that from the constant weights strategy ( $\hat{b} = 10$ ). We observe

Training with Expected Blocksize $\hat{b} = 10$ years: Market Cap Weighted					
Strategy	$E(W_T)$	$std(W_T)$	$median(W_T)$	$Pr(W_T) < 500$	$Pr(W_T < 600)$
Expected Blocksize $\hat{b} = 0.5$ years					
constant proportion ( $p = (0.6, 0.1, 0.3)$ )	860	450	758	0.18	0.31
NN adaptive	794	216	934	0.14	0.20
Expected Blocksize $\hat{b} = 1$ years					
constant proportion ( $p = (0.6, 0.1, 0.3)$ )	857	429	761	0.18	0.30
NN adaptive	798	215	941	0.14	0.19
Expected Blocksize $\hat{b} = 2$ years					
constant proportion ( $p = (0.6, 0.1, 0.3)$ )	849	414	758	0.18	0.30
NN adaptive	801	205	935	0.13	0.18
Expected Blocksize $\hat{b} = 5$ years					
constant proportion ( $p = (0.6, 0.1, 0.3)$ )	841	383	769	0.17	0.29
NN adaptive	812	195	941	0.11	0.17
Expected Blocksize $\hat{b} = 8$ years					
constant proportion ( $p = (0.6, 0.1, 0.3)$ )	827	350	769	0.16	0.28
NN adaptive	821	185	941	0.10	0.15
Expected Blocksize $\hat{b} = 10$ years					
constant proportion ( $p = (0.6, 0.1, 0.3)$ )	826	337	772	0.16	0.27
NN adaptive	826	180	941	0.09	0.14

TABLE 16: *Performance comparisons using the cap-weighted index, 3-month T-bill and i 10-year treasury: the last data set with the expected blocksize  $\hat{b} = 10$  years is the training set. Test performance comparisons are reported on the remaining data sets.*

Training with Expected Blocksize $\hat{b} = 0.5$ years: Equal Weighted					
Strategy	$E(W_T)$	$std(W_T)$	$median(W_T)$	$Pr(W_T) < 700$	$Pr(W_T < 900)$
Expected Blocksize $\hat{b} = 0.5$ years					
constant proportion ( $p = (0.6, 0.1, 0.3)$ )	1152	792	950	0.30	0.46
NN adaptive	1152	398	1351	0.19	0.26
Expected Blocksize $\hat{b} = 1$ years					
constant proportion ( $p = (0.6, 0.1, 0.3)$ )	1152	789	950	0.29	0.46
NN adaptive	1153	398	1352	0.19	0.26
Expected Blocksize $\hat{b} = 2$ years					
constant proportion ( $p = (0.6, 0.1, 0.3)$ )	1079	594	945	0.27	0.46
NN adaptive	1174	358	1327	0.15	0.23
Expected Blocksize $\hat{b} = 5$ years					
constant proportion ( $p = (0.6, 0.1, 0.3)$ )	1034	456	952	0.23	0.45
NN adaptive	1203	321	1327	0.11	0.19
Expected Blocksize $\hat{b} = 8$ years					
constant proportion ( $p = (0.6, 0.1, 0.3)$ )	1012	398	954	0.21	0.44
NN adaptive	1215	301	1327	0.09	0.17
Expected Blocksize $\hat{b} = 10$ years					
constant proportion ( $p = (0.6, 0.1, 0.3)$ )	1007	376	961	0.21	0.43
NN adaptive	1227	288	1334	0.08	0.16

TABLE 17: *Performance comparisons using the equal-weighted index, 3-month T-bill and 10-year treasury: the first data set with the expected blocksize  $\hat{b} = 0.5$  years is the training set. Test performance comparisons are reported on the remaining data sets.*

Training with Expected Blocksize $\hat{b} = 10$ years: Equal Weighted					
Strategy	$E(W_T)$	$std(W_T)$	$median(W_T)$	$Pr(W_T) < 700$	$Pr(W_T < 900)$
Expected Blocksize $\hat{b} = 0.5$ years					
constant proportion ( $p = (0.6, 0.1, 0.3)$ )	1152	792	950	0.30	0.46
NN adaptive	929	245	1075	0.18	0.27
Expected Blocksize $\hat{b} = 1$ years					
constant proportion ( $p = (0.6, 0.1, 0.3)$ )	1152	789	950	0.29	0.46
NN adaptive	931	245	1075	0.18	0.26
Expected Blocksize $\hat{b} = 2$ years					
constant proportion ( $p = (0.6, 0.1, 0.3)$ )	1079	594	945	0.27	0.46
NN adaptive	959	209	1075	0.13	0.22
Expected Blocksize $\hat{b} = 5$ years					
constant proportion ( $p = (0.6, 0.1, 0.3)$ )	1034	456	952	0.23	0.45
NN adaptive	987	176	1075	0.09	0.18
Expected Blocksize $\hat{b} = 8$ years					
constant proportion ( $p = (0.6, 0.1, 0.3)$ )	1012	398	954	0.21	0.44
NN adaptive	1001	157	1075	0.07	0.15
Expected Blocksize $\hat{b} = 10$ years					
constant proportion ( $p = (0.6, 0.1, 0.3)$ )	1007	376	961	0.21	0.43
NN adaptive	1007	146	1075	0.06	0.14

TABLE 18: *Performance comparisons using the equal-weighted index, 3-month T-bill and 10-year treasury: the last data set with the expected blocksize  $\hat{b} = 10$  years is the training set. Test performance comparisons are reported on the remaining data sets.*

514 that, from these distributions, the performance of the NN control dominates that of the constant strategy in  
515 three-asset cases. We also note that here the test performance, which corresponds to a larger blocksize, has  
516 a better performance than the training data set, likely due to serial correlations.

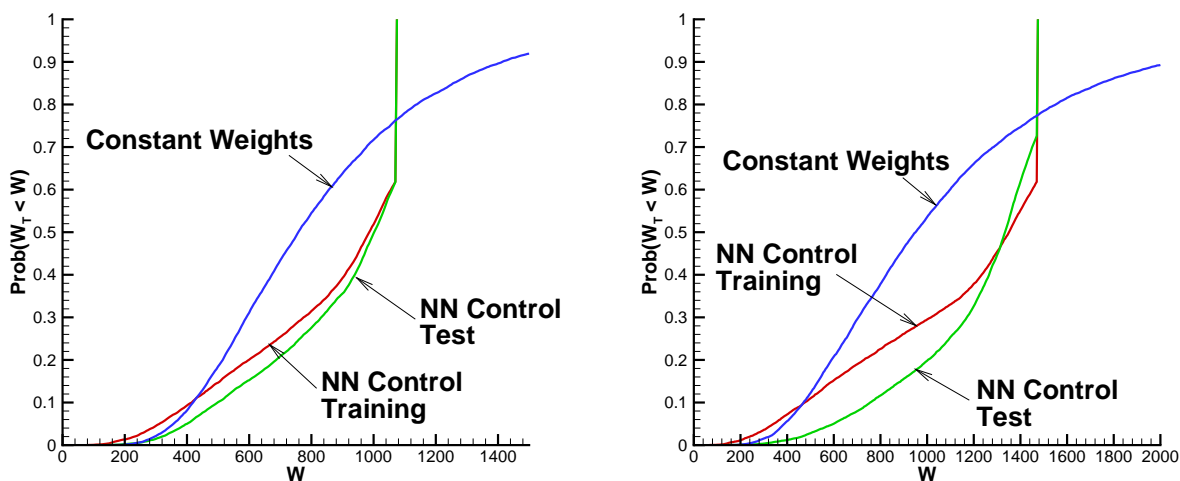
## 517 9 Conclusions

518 If realistic constraints are applied to a DC pension plan asset allocation policy (e.g. no leverage, no shorting,  
519 discrete rebalancing), then in order to determine the optimal control, the HJB equation must be solved  
520 numerically. Solving a multistage stochastic optimal investment problem is challenging when the number of  
521 state variables becomes large, since the curse of dimensionality comes into play when using the HJB PDE.  
522 In addition, a PDE method requires a parametric stochastic model to be specified and calibrated to market  
523 data. This is the dominant approach used computational finance for the last few decades.

524 In this paper, we consider solving the multi-stage optimal decision problem arising from a finite number  
525 of scenarios. When the set of scenarios are i.i.d. samples of a parametric stochastic model, the scenario  
526 optimization problem is an approximation to the parametric model based optimization problem. If the  
527 scenarios are market price observations (or generated from a resampling approach), solving the scenario  
528 optimization directly for the controls leads to a market data driven optimal investment strategy. The resulting  
529 scenario optimization problem is large since the number of unknowns is  $O(NLM)$ , where  $N$  is the number  
530 of periods,  $M$  is the number of assets and  $L$  is the number of scenario paths.

531 Instead of following a backward timestepping process using Bellman's principle to tackle the multi-stage  
532 stochastic optimization problem, we propose to solve the large scale scenario optimization problem directly.  
533 To overcome the challenge of a large dimensional optimization problem, we propose using a parsimonious  
534 NN model to represent the control at all different rebalancing times, using the features of current wealth and  
535 time-to-go as the inputs to the NN model. The resulting optimization problem has a dimension  $O(l(d+M))$ ,  
536 where  $l$  is the number of hidden nodes,  $d$  is the number of features, and  $M$  is the number of assets.

537 We first validate the proposed NN optimization approach by comparing the training performance with  
538 the benchmark strategy computed by solving an HJB PDE equation, assuming a parametric market model.



(a) Cap-weighted CRSP, 3 month T-bill, 10 year Treasury

(b) Equal-weighted CRSP, 3 month T-bill, 10 year Treasury.

FIGURE 4: Comparison of the cumulative distribution functions for the control computed using Neural Network (NN) and constant strategy. The constant weight strategy is  $p = (0.6, 0.1, 0.3)$ . Surplus cash is not included in the distribution functions for the NN controls.

539 The HJB solution generates the provably optimal strategy in this case. Our computational results (using the  
 540 parametric model) demonstrate that, using a parsimonious 2-layer NN with three hidden nodes, we obtain  
 541 performance on par with that from the optimal HJB control. This validation is conducted for a 2-asset base  
 542 case, with two portfolio composition scenarios: a cap-weighted real CRSP index and real 3-month T-bill,  
 543 and an alternative case with an equal-weighted real CRSP index and real 10-year treasury.

544 In addition, we report test performance of the NN control on the bootstrap resampling market data sets  
 545 and observe performance comparison similar to the training based on simulated model scenarios. This  
 546 demonstrates robustness of the learned NN controls.

547 The proposed method provides a way of learning controls directly from the market data without first  
 548 estimating a parametric model. To investigate this, we learn NN controls from bootstrap resamples of  
 549 the historical market data, with different expected block sizes, and examine both the training performance  
 550 comparisons and test performance comparisons on the parametric market model data sets. We observe  
 551 that the NN optimal controls from the market data sets generate superior training and testing performances  
 552 compared to that of the constant proportion strategies, at a similar level to the parametric model based HJB  
 553 method.

554 In addition, we also consider 3-asset investment problems with two choices of assets: (i) a cap-weighted  
 555 CRSP index, 3-month bill and 10-year treasury or (ii) an equal-weighted CRSP index, 3-month bill and  
 556 10-year treasury. We observe similar levels of training and test improvement from the NN controls over  
 557 those of the constant proportion 60:10:30 strategy.

558 Overall, the performance of the NN dynamically adaptive strategy significantly dominates that of the  
 559 constant proportion strategies, achieving higher median values of the terminal wealth, and smaller probabil-  
 560 ities of shortfall, compared with the constant weight strategies.

561 One main technical question which arises is the choice of block size to be used for training the NN  
 562 control. If we believe that serial correlation is important going forward, then use of a larger block size  
 563 would be recommended. On the other hand, a smaller block size would be appropriate if we view the  
 564 processes as essentially i.i.d. We use a joint resampling process, where we use the same block size for



565 all the components of the portfolio. This preserves the historical correlations amongst the components of  
566 the portfolio. However, it is not clear how to select an optimal blocksize in this situation. We intend to  
567 investigate the choice of blocksize in the context of NN training with bootstrap resampling in the future. For  
568 now, we suggest the conservative approach of using a small blocksize, since this seems to be quite robust.

569 We remark that the proposed NN optimization framework makes it computationally feasible to solve  
570 problems with a larger number of assets, and without specifying a parametric market model. Although we  
571 have focused on a DC pension plan example, it is straightforward to apply these techniques to other objective  
572 functions. For example, a problem of much current interest is optimal asset allocation for defined benefit  
573 (DB) plans, with the objective function being to minimize shortfall with respect to a target funding ratio.

## 574 **10 Acknowledgments**

575 This research was supported in part by the Natural Sciences and Engineering Research Council of Canada  
576 (NSERC) grants: RGPIN-2017-03760 and RGPIN-2014-03978. The authors have no conflicts of interest to  
577 report.

## 578 **References**

579 Basak, S. and G. Chabakauri (2010). Dynamic mean-variance asset allocation. *Review of Financial Stud-*  
580 *ies* 23, 2970–3016.

581 Bauerle, N. and S. Grether (2015). Complete markets do not allow free cash flow streams. *Mathematical*  
582 *Methods of Operations Research* 81, 137–146.

583 Bertsekas, D. P. and J. N. Tsitsiklis (1996). *Neuro-dynamic Programming*. Belmont, Massachusetts: Athena  
584 Scientific.

585 Bjork, T., A. Murgoci, and X. Zhou (2014). Mean variance portfolio optimization with state dependent risk  
586 aversion. *Mathematical Finance* 24, 1–24.

587 Cogneau, P. and V. Zakalmouline (2013). Block bootstrap methods and the choice of stocks for the long  
588 run. *Quantitative Finance* 13, 1443–1457.

589 Coleman, T. and Y. Li (1996). An interior, trust region approach for nonlinear minimization subject to  
590 bounds. *SIAM Journal on Optimization* 6, 418–445.

591 Cong, F. and C. Oosterlee (2016). Multi-period mean variance portfolio optimization based on Monte-Carlo  
592 simulation. *Journal of Economic Dynamics and Control* 64, 23–38.

593 Cont, R. and C. Mancini (2011). Nonparametric tests for pathwise properties of semimartingales.  
594 *Bernoulli* 17, 781–813.

595 Dang, D.-M. and P. Forsyth (2016). Better than pre-commitment mean-variance portfolio allocation strate-  
596 gies: a semi-self-financing Hamilton-Jacobi-Bellman equation approach. *European Journal of Opera-*  
597 *tional Research* 250, 827–841.

598 Dang, D. M. and P. A. Forsyth (2014). Continuous time mean-variance optimal portfolio allocation un-  
599 der jump diffusion: A numerical impulse control approach. *Numerical Methods for Partial Differential*  
600 *Equations* 30, 664–698.

601 Dichtl, H., W. Drobetz, and M. Wambach (2016). Testing rebalancing strategies for stock-bond portfolios  
602 across different asset allocations. *Applied Economics* 48, 772–788.

603 Donnelly, C., R. Gerrard, M. Gullen, and J. Nielsen (2015). Less is more: increasing retirement gains by  
604 using an upside terminal wealth constraint. *Insurance: Mathematics and Economics* 64, 259–267.

605 Forsyth, P. and G. Labahn (2018).  $\epsilon$ -monotone Fourier methods for optimal stochastic control in finance. to  
606 appear, *Journal of Computational Finance*.

607 Gan, G. (2013). Application of data clustering and machine learning in variable annuity valuation. *Insur-*  
608 *ance: Mathematics and Economics* 53, 795–801.

609 Gan, G. and X. Lin (2015). Valuation of large variable annuity portfolios under nested simulation: a func-  
610 tional data approach. *Insurance: Mathematics and Economics* 62, 138–150.

611 Gu, S., R. Kelly, and D. Xu (2018). Empirical asset pricing via machine learning. SSRN:3159577.

612 Guan, G. and Z. Liang (2015). Mean-variance efficiency of DC pension plan under stochastic interest rate  
613 and mean-reverting returns. *Insurance: Mathematics and Economics* 61, 99–109.

614 He, L. and Z. Liang (2013). Optimal investment strategy for the DC plan with return of premiums clauses  
615 in a mean-variance framework. *Insurance: Mathematics and Economics* 53, 643–649.

616 Hejazi, S. and K. Jackson (2016). A neural network approach to efficient valuation of large portfolios of  
617 variable annuities. *Insurance: Mathematics and Economics* 70, 169–181.

618 Homer, S. and R. Sylla (2005). *A History of Interest Rates*. New York: Wiley.

619 Kou, S. and H. Wang (2004). Option pricing under a double exponential jump diffusion model. *Management*  
620 *Science* 50, 1178–1192.

621 Kou, S. G. (2002). A jump-diffusion model for option pricing. *Management Science* 48, 1086–1101.

622 Li, D. and W.-L. Ng (2000). Optimal dynamic portfolio selection: Multiperiod mean-variance formulation.  
623 *Mathematical Finance* 10, 387–406.

624 Lioui, A. (2013). Time consistent vs. time inconsistent dynamic asset allocation: some utility cost calcula-  
625 tions for mean variance preferences. *Journal of Economic Dynamics and Control* 37, 1066–1096.

626 Menoncin, F. and E. Vigna (2017). Mean-variance target based optimisation for defined contribution pension  
627 schemes in a stochastic framework. *Insurance: Mathematics and Economics* 76, 172–184.

628 Patton, A., D. Politis, and H. White (2009). Correction to: Automatic block-length selection for the depen-  
629 dent bootstrap. *Econometric Reviews* 28, 372–375.

630 Politis, D. and H. White (2004). Automatic block-length selection for the dependent bootstrap. *Econometric*  
631 *Reviews* 23, 53–70.

632 Vigna, E. (2014). On efficiency of mean-variance based portfolio selection in defined contribution pension  
633 schemes. *Quantitative Finance* 14, 237–258.

634 Vigna, E. (2017). Tail optimality and preferences consistency for intertemporal optimization problems.  
635 Working papers, Collegio Carlo Alberto, Università di Torino.

- 636 Vinyals, O., T. Edwards, S. Bartunov, P. Georgiev, A. S. Vezhnevets, M. Yeo, A. Makhzani, H. Kürtler,  
637 J. Agapiou, J. Schrittwieser, J. Quan, S. Gaffney, S. Petersen, K. Simonyan, T. Schaul, H. van Hasselt,  
638 D. Silver, T. Lillicrap, K. Calderone, P. Keet, A. Brunasso, D. Lawrence, A. Ekeremo, J. Repp, and R. Tsing  
639 (2017). StarCraft II a new challenge for reinforcement learning. arXiv:1708.04782.
- 640 Wu, H., L. Zhang, and H. Chen (2015). Nash equilibrium strategies for a defined contribution pension  
641 management. *Insurance: Mathematics and Economics* 62, 202–214.
- 642 Yao, H., Z. Yang, and P. Chen (2013). Markowitz’s mean-variance defined contribution pension fund man-  
643 agement under inflation: A continuous time model. *Insurance: Mathematics and Economics* 53, 851–863.
- 644 Zhou, X. Y. and D. Li (2000). Continuous-time mean-variance portfolio selection: A stochastic LQ frame-  
645 work. *Applied Mathematics and Optimization* 42, 19–33.